Modulation of electronic properties of monolayer InSe through strain and external electric field

Doan Q. Khoa[a,b], Duy Trinh Nguyen[c], Chuong V. Nguyen[d,*], Vo T.T. Vi[e,f], Huynh V. Phuc[g], Le T.T. Phuong[e], Bui D. Hoi[e], Nguyen N. Hieu[h,*]

[a] Division of Computational Physics, Institute for Computational Science, Ton Duc Thang University, Ho Chi Minh City, Viet Nam
[b] Faculty of Electrical and Electronics Engineering, Ton Duc Thang University, Ho Chi Minh City, Viet Nam
[c] NTT Institute of Hi-Technology, Nguyen Tat Thanh University, Ho Chi Minh City, Viet Nam
[d] Department of Materials Science and Engineering, Le Quy Don Technical University, Ha Noi, Viet Nam
[e] Department of Physics, University of Education, Hue University, Hue, Viet Nam
[f] Department of Fundamental Sciences, University of Medicine and Pharmacy, Hue University, Hue, Viet Nam
[g] Division of Theoretical Physics, Dong Thap University, Dong Thap, Viet Nam
[h] Institute of Research and Development, Duy Tan University, Da Nang, Viet Nam

A B S T R A C T

In this work, we consider systematically the influence of uniaxial strain and external electric field E on electronic properties of a monolayer InSe using *ab initio* approach based on density functional theory. Our calculations indicate that the monolayer InSe has a medium indirect energy bandgap of 1.38 eV at equilibrium. The calculated results also demonstrate that we can adjust the bandgap of the monolayer InSe by strain engineering or electric field. The bandgap of the monolayer InSe changes dramatically when the uniaxial strain is applied. Especially, under the compressed uniaxial strain, an indirect–direct bandgap transition has been observed at certain elongations. Within the electric field magnitude E range from 0 to 5 V/nm, the calculated results show that the negative electric field changes the bandgap of the monolayer InSe up to 23% while the positive electric field effect on its bandgap is negligible.

1. Introduction

Since the experimentally discovery by Novoselov and co-workers in 2004 [1], graphene has been one of the most research-intensive materials. Success in graphene research is a very positive motivation for scientists to study other layered materials, both theoretically and experimentally [2–9]. Recently, other novel two-dimensional (2D) materials have been discovered, including monolayers of transition metal dichalcogenides [10] and monochalcogenides [11]. Among them, the monochalcogenides come out as materials that have many applications in optoelectronic and nanoelectromechanical devices [12–14]. The monochalcogenides have a large natural bandgap, which overcomes the disadvantage of graphene whose bandgap is zero. In the present work, we focus on the 2D monolayer InSe material which has been recently successfully synthesized [15,16]. The InSe monolayer with very high carrier mobility [17], strong charge transfer [18], and broad absorption spectrum [19] might be a potential candidate for applications in nanoelectronic and optoelectronic devices.

Bulk InSe has a bandgap of 0.41 eV obtained by density functional theory (DFT) calculations [17], and the band gap of the InSe material depends strongly on its thickness or the number of layers [20,21], especially an indirect-direct transition can occur with decreasing the number of layers of the sample [22]. In the monolayer form, the geometry structure of InSe belongs to the D_{3h} group-space and its crystal structure is stable because the phonon spectrum does not have imaginary frequencies [23]. Also, the monolayer InSe has outstanding mechanical flexibility. Previous DFT calculations have been indicated that the critical uniaxial strain along the zigzag (armchair) direction of the monolayer InSe is up to 25% (27%) [24]. In addition, based on the calculations of the Young's modulus and strain–stress relations, Hu and co-workers [24] predicted that the strain threshold of the monolayer InSe is close to that of other two-dimensional layered materials such as phosphorene which is stable under applied strain from −16% to 20% [25] or monolayer SnS exhibits a superior mechanical stability with compression strain threshold is up to −20% [26]. Using DFT calculations, Demirci and co-workers showed that the monolayer InSe is a

semiconductor with an indirect energy bandgap of 1.37 eV at equilibrium [23]. However, the indirect–direct bandgap transition may occur when the structure is deformed, and it becomes a direct semiconductor at proper elongations of the strain [24]. Besides, Wang and co-workers indicated that, an electric field can enhance the mobility of carriers and, in particular, increase the intensity of the absorption of gas molecules [27]. This character of the monolayer InSe is especially useful for applications in gas sensors. Besides, the appearance of ferromagnetic/antiferromagnetic ground states in the $3d$ transition metal-doped monolayer InSe systems [28] is expected to have many applications in spintronics. Recently, van der Waals heterostructures based on InSe have attracted many research groups [29–33]. DFT calculations showed that, although the bound between the graphene and monolayer InSe is very weak, a tiny energy bandgap appears in the graphene/InSe heterostructure because of the sublattice symmetry breaking [32]. Although above-mentioned efforts, the electronic properties of the monolayer InSe have been not understood completely, especially under external conditions, and need to be investigated further.

In the present work, we study systematically the electronic properties of the monolayer InSe in the presence of the uniaxial strain and external electric field (E) using DFT calculations. Our work focuses mainly on the influence of the strain engineering and the electric field on the band structure and energy bandgap of the structure. Discussions on the phase transition and the influence of E on the electronic properties of the monolayer InSe are also addressed in this work.

2. Model and computational details

In the present study, all the calculations of the structural parameters and electronic properties of the monolayer InSe are performed by the *ab initio* calculations based on the DFT, which was implemented by the Quantum Espresso package [34] with accurate projector augmented-wave (PAW) pseudopotentials [35,36] and the Perdew-Burke-Ernzerhof (PBE) exchange–correlation energy functional [37,38]. In addition, in order to describe exactly the van der Waals interactions, which may exist between In and Se layers, we use the DFT-D2 with London dispersion corrections as proposed by Grimme (PBE + D2) [39]. The first Brillouin zone (BZ) is sampled with $(15 \times 15 \times 1)$ k-mesh Monkhorst–Pack grid. We use 500 eV as the cut-off of kinetic energy for plane-wave basis in our numerical calculations. The monolayer InSe structure is fully relaxed with convergence criteria for the force acting on each atom and the total energy being 0.01 eV/Å and 10^{-6} eV, respectively. In order to avoid the interactions between neighboring slabs, a vacuum space of 20 Å in the z direction is used.

To evaluate the influence of the uniaxial strain on the electronic properties of the monolayer InSe, the elongation of the uniaxial strain ε can be defined via the lattice constants as $\varepsilon = (\delta - \delta_0)/\delta_0$, where δ_0 and δ are the equilibrium and strained lattice constants of the monolayer InSe, respectively. The external electric field in this study is applied perpendicularly to the monolayer InSe plane (along z-axis as shown in Fig. 1).

3. Results and discussion

In Fig. 1, we show the atomic structure of the monolayer InSe at the equilibrium state. It is well-known that the structure of the monolayer InSe belongs to the D_{3h} space group [23]. Our calculations indicate that the optimized lattice constants of the monolayer InSe at the equilibrium are $a = b = 3.89$ Å and the In–Se bond length $d_{\text{In--Se}}$ and the In–In bond length $d_{\text{In--In}}$ are, respectively, 2.58 Å and 2.81 Å. The thickness of the monolayer InSe at the equilibrium state is 5.35 Å. These computed results are close to those in the previous theoretical studies [23,40]. In this paper, the uniaxial strains from −15% to 15% were included in the calculation. The minus sign refers to the compression strain. Our calculations indicate that the In–Se bond length decreases from 2.58 Å to 2.436 Å when the compression strain varies from 0 to −15 %, whereas it increases from 2.58 Å up to 2.73 Å when the tensile strain is increased from 0 up to 15 %, respectively. At the equilibrium state, the monolayer InSe is an indirect semiconductor and its energy gap is 1.38 eV. From Fig. 2, we can see that the highest subband in the valence band (near the Fermi level) has two maxima which are symmetric across the vertical line passing across the S-point. The indirect bandgap is formed from the lowest point of the conduction band at the S-point and one of these two maxima as shown in Fig. 2(d). However, in this subband of the valence band, the difference in energy between these two maxima and the point just above the S-point is very small. Therefore, with sensitivity to external conditions, we expect that this subband can be changed leading to the indirect–direct energy gap transition in the monolayer InSe due to strain or external electric field.

In Fig. 2, we show the computational results for the band structure of the monolayer InSe in the presence of the uniaxial strain. In this investigation, we perform the calculations for the uniaxial strains along both directions in the plane of the 2D monolayer, i.e., the applied uniaxial strain along the armchair ε_{ac} (AC-strain) and the zigzag ε_{zz} (ZZ-strain) directions. We find that, compared to the case of absence of the strain, the positions of the valence band maximum (VBM) and the conduction band minimum (CBM) are unchanged in the presence of the tensile strains. Meanwhile, the effect of compression strains (in both directions) on the band structure of the monolayer InS is very strong. In fact, as we expected above, the compression strains change the position of the VBM and lead to an indirect–direct bandgap transition as shown in Fig. 2(c) in the case of the compression ZZ-strain $\varepsilon_{zz} < 0$ and in Fig. 2(h,i,j) in the case of $\varepsilon_{ac} < 0$. In these cases, we see that the compression strains not only alter significantly the shape of the highest subband of the valence band, but also the position of the VBM. As we can see in Fig. 2(h,i,j), under the compression AC-strain $\varepsilon_{ac} < 0$, the VBM shifts to the point S whearea the CBM remains unchanged from the equilibrium state. Thus, the monolayer InSn becomes a direct semiconductor with a medium bandgap opening at the S-point when the compression AC-strain is presented. However, in the case of the compression ZZ-strain, the monolayer InS is a semiconductor only when the elongation of the ZZ-strain ε_{ac} is around −5% because the compression ZZ-strain changes both the VBM and the CBM. Our detailed
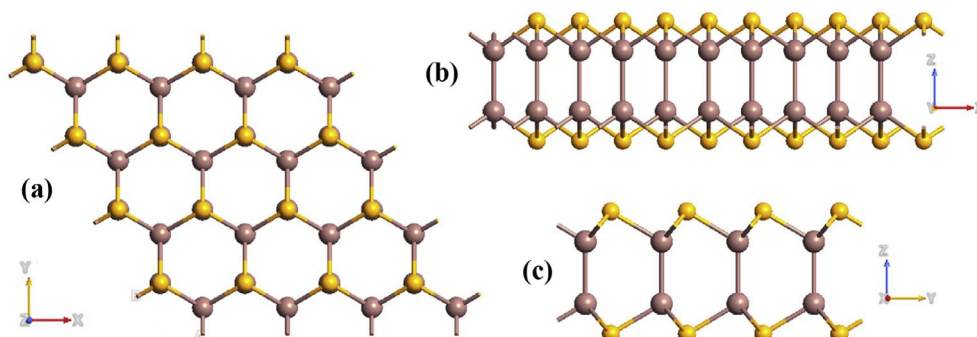
Fig. 1. (a) Top view, (b) side view, and (c) front view of the atomic configuration of monolayer InSe.
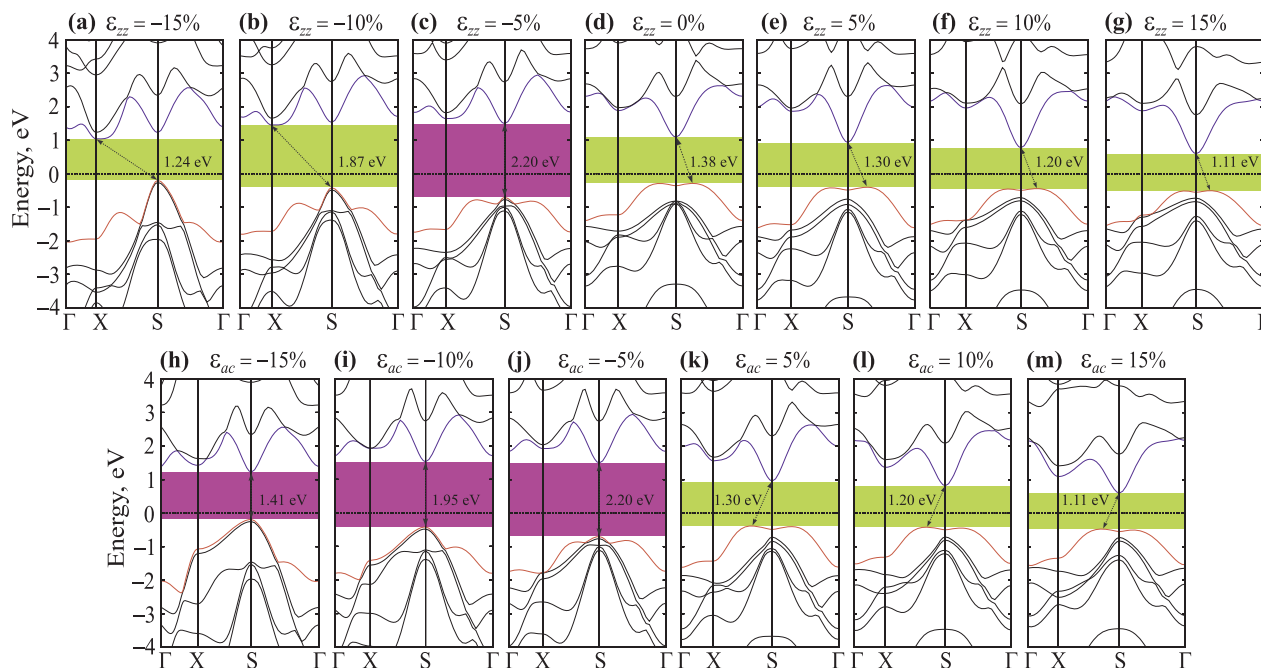
Fig. 2. (a) Band structure of the monolayer InSe under uniaxial strains along the zigzag direction (a) $\varepsilon_{zz} = -15\%$, (b) $\varepsilon_{zz} = -10\%$, (c) $\varepsilon_{zz} = -5\%$, (d) $\varepsilon_{zz} = 0\%$ (at equilibrium), (e) $\varepsilon_{zz} = 5\%$, (f) $\varepsilon_{zz} = 10\%$, (g) $\varepsilon_{zz} = 15\%$ and along the armchair direction (h) $\varepsilon_{ac} = -15\%$, (i) $\varepsilon_{ac} = -10\%$, (j) $\varepsilon_{ac} = -5\%$, (k) $\varepsilon_{ac} = 5\%$, (l) $\varepsilon_{ac} = 10\%$, and (m) $\varepsilon_{ac} = 15\%$.
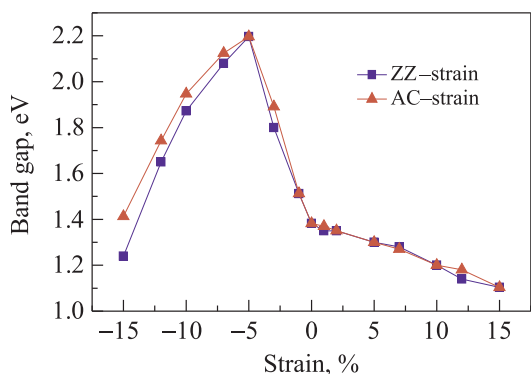
Fig. 3. Dependence of the energy bandgap of the monolayer on uniaxial strains.

calculations show that when $\varepsilon_{zz} > 5\%$, while the position of the VBM changes and locates at the S-point, the position of the CBM moves to the X-point as shown in Fig. 2(a,b). Thus, the indirect–direct bandgap transition in the presence of the compression ZZ-strain occurs only when the ε_{zz} is around 5%. On the other hand, while the electronic energy band structure of the monolayer InSe is greatly altered by the compression strains, it is quite stable under the tensile strains in both directions. In the presence of the tensile strains, there is no indirect–direct bandgap transition and the change of bandgap is quite small. The dependence of the energy bandgap of the monolayer InSe on the uniaxial strains is shown in Fig. 3.

To estimate the effect of the uniaxial strains on the bandgap, we calculate for the strains along both directions of the lattice plane. We can see that, from Fig. 3, the difference between strain directions, i.e., ZZ-strain and AC-strain, is negligible. The bandgap decreases linearly as the tensile strain increases. However, this decrease is quite small, about 20% with the strain varied from 0 to 15%. In contrast, under the compression strain the bandgap increases (compared to the equilibrium state), reaches a maximum at the elongation of -5% and then decreases with increasing continuously the compression strain. The law of the bandgap change versus the uniaxial strain in the monolayer InSe in the

present study is in good agreement with the previous first-principles calculations by Jin and co-workers [40].

To have a deeper insight to the effect of uniaxial strains on the electronic structure of the monolayer InSe, we investigate its partial density of states (DOS) under strain as shown in Fig. 4. We can see that the valence band is significantly contributed by the Se-p and In-d orbitals. The contribution of the Se-p orbitals to the valence band is predominant while the conduction band receives more contribution from the In-d orbitals. The contribution of the In-d orbitals to both the valence and conduction bands is roughly the same. In particular, the uniaxial strains (both compression and tensile cases) increases the contribution of In-d orbitals and reduces the contribution of Se-p orbitals to the conduction band of the monolayer InSe. The contribution of the s-Se and In-p orbitals to the electronic band of the material is quite small compared to that of the Se-p and In-d orbitals. Fig. 5.

It is well-known that 2D materials, such as hexagonal boron nitride, graphene or monochalcogenides, are very sensitive to external conditions. Along with strain engineering, using external electric fields is one of the easiest ways to control their electronic properties. In the following, we perform an examination on the effect of an external electric field on the band structure and energy bandgap of the monolayer InSe. The electric field E is applied perpendicularly to the 2D surface of the monolayer (along the z-axis). It implies that the direction of the electric field coincides with the positive direction of the z-axis. In Fig. 6, we demonstrate the effect of the electric field E (with two opposite directions of the electric field denoting by signs "+" and "−") on the band structure of the monolayer InSe. Our calculations demonstrate that, within the limit of electric field magnitude E from 0 to 5 V/nm, there is no indirect–direct transition occurring in the monolayer InSe. The dependence of the energy bandgap of the monolayer InSe on the external electric field is illustrated in Fig. 6. We can see that, the bandgap of the monolayer InSe is almost unchanged when the magnitude of the applied electric field is in the range of 0 to 5 V/nm. Interestingly, while the positive field does not change much the energy bandgap, the bandgap of the monolayer InSe depends strongly on the negative electric field (the electric field direction is opposite to that of the z axis), especially at the large negative electric field. The bandgaps of the

(a)

Tensile ZZ-strain   Compressive ZZ-strain

(b)

Tensile AC-strain   Compressive AC-strain
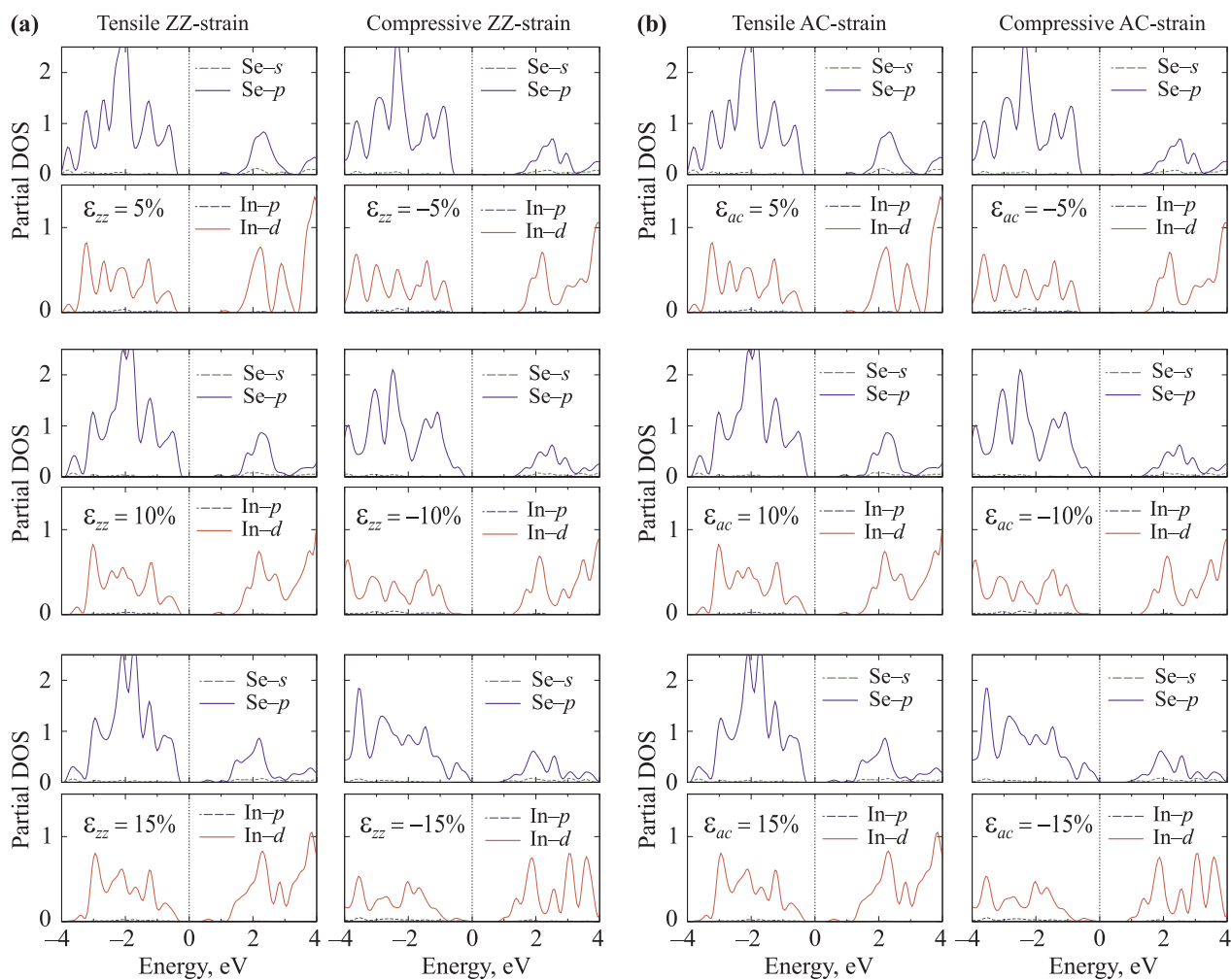
Fig. 4. Partial DOS of the monolayer InSe under (a) ZZ-strain ε_{zz} and (b) AC-strain ε_{ac}.

monolayer InSe at $E = 5$ V/nm and $E = -5$ V/nm are, respectively, 1.37 eV and 1.06 eV. Compared to the equilibrium (1.38 eV), the positive electric field of $E = 5$ V/nm reduces only 0.4% of the bandgap while the negative electric field of $E = -5$ V/nm reduces it up to 23%. This difference is due to the location of the orbital and differences in vacuum spaces of the upper and lower face of the monolayer InSe. The modulation of electronic properties of the monolayer InSe by the external electric field is important for prospective applications in nanodevices based on electric field effect.

4. Conclusion

In summary, using the DFT calculations we have investigated the electronic properties of the monolayer InSe under uniaxial strain and external electric field. Our DFT calculations demonstrate that the electronic properties of the monolayer InSe depend strongly on the uniaxial strains, especially in the compression case. The compression uniaxial strain not only drastically changes the electronic energy band structure, but also leads to the indirect–direct bandgap transition in the
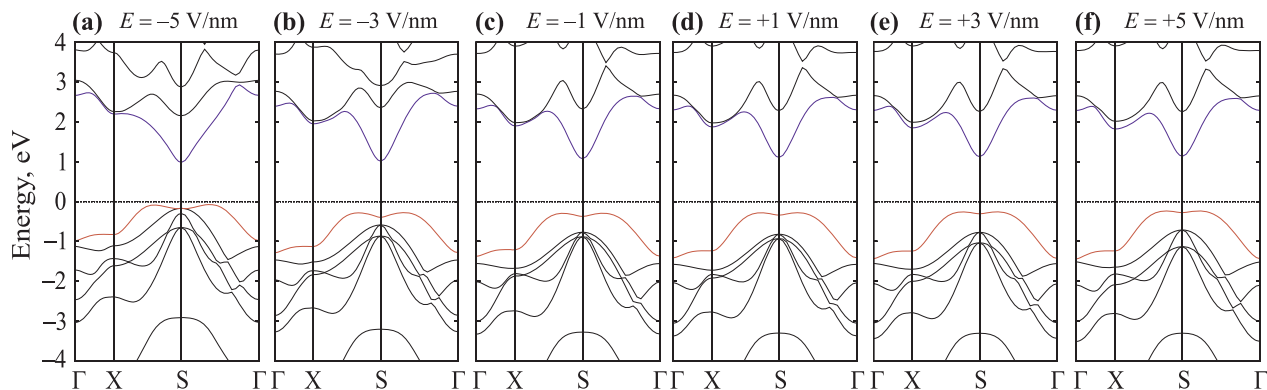
Fig. 5. Band structure of the monolayer InSe under the electric field E: (a) $E = -5$ V/nm, (b) $E = -3$ V/nm, (c) $E = -1$ V/nm, (d) $E = +1$ V/nm, (e) $E = +3$ V/nm, and (f) $E = +5$ V/nm.
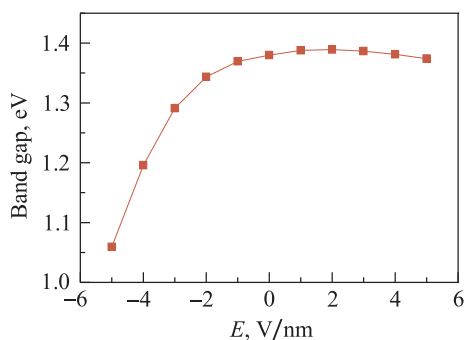
Fig. 6. Dependence of the bandgap of the monolayer InSe on electric field E.

monolayer InSe. Our DFT calculations also indicated that the valence and conduction bands are mainly contributed by the Se-p and In-d orbitals. However, the uniaxial strain increases the contribution of the In-d and reduces the contribution of Se-p orbitals to the conduction band of the monolayer InSe. In addition, the possibility of controlling the energy gap using the external electric field in the monolayer InSe makes the material becoming a potential candidate for nanoelectronic and optoelectronic applications.

Acknowledgment

References

[1] K.S. Novoselov, A.K. Geim, S.V. Morozov, D. Jiang, Y. Zhang, S.V. Dubonos, I.V. Grigorieva, A.A. Firsov, Science 306 (2004) 666.
[2] A.I. Siahlo, N.A. Poklonski, A.V. Lebedev, I.V. Lebedeva, A.M. Popov, S.A. Vyrko, A.A. Knizhnik, Y.E. Lozovik, Phys. Rev. Mater. 2 (2018) 036001.
[3] C.V. Nguyen, N.N. Hieu, N.A. Poklonski, V.V. Ilyasov, L. Dinh, T.C. Phong, L.V. Tung, H.V. Phuc, Phys. Rev. B 96 (2017) 125411.
[4] H.V. Phuc, N.N. Hieu, B.D. Hoi, C.V. Nguyen, Phys. Chem. Chem. Phys. 20 (2018) 17899.
[5] V.V. Ilyasov, C.V. Nguyen, I.V. Ershov, C.D. Nguyen, N.N. Hieu, Mater. Chem. Phys. 154 (2015) 78.
[6] N.N. Hieu, H.V. Phuc, V.V. Ilyasov, N.D. Chien, N.A. Poklonski, N. Van Hieu, C.V. Nguyen, J. Appl. Phys. 122 (10) (2017) 104301.
[7] J.R. Brent, N. Savjani, E.A. Lewis, S.J. Haigh, D.J. Lewis, P. O'Brien, Chem. Commun. 50 (2014) 13338.
[8] C.V. Nguyen, N.N. Hieu, C.A. Duque, D.Q. Khoa, N.V. Hieu, L.V. Tung, H.V. Phuc, J. Appl. Phys. 121 (2017) 045107.
[9] H.V. Phuc, V.V. Ilyasov, N.N. Hieu, B. Amin, C.V. Nguyen, J. Alloys Compd. 750 (2018) 765.
[10] J.N. Coleman, M. Lotya, A. O'Neill, S.D. Bergin, P.J. King, U. Khan, K. Young, A. Gaucher, S. De, R.J. Smith, I.V. Shvets, S.K. Arora, G. Stanton, H.-Y. Kim, K. Lee, G.T. Kim, G.S. Duesberg, T. Hallam, J.J. Boland, J.J. Wang, J.F. Donegan, J.C. Grunlan, G. Moriarty, A. Shmeliov, R.J. Nicholls, J.M. Perkins, E.M. Grieveson, K. Theuwissen, D.W. McComb, P.D. Nellist, V. Nicolosi, Science 331 (2011) 568.
[11] P. Hu, L. Wang, M. Yoon, J. Zhang, W. Feng, X. Wang, Z. Wen, J.C. Idrobo, Y. Miyamoto, D.B. Geohegan, K. Xiao, Nano Lett. 13 (2013) 1649.
[12] W. Feng, X. Zhou, W.Q. Tian, W. Zheng, P. Hu, Phys. Chem. Chem. Phys. 17 (2015) 3653.
[13] D.J. Late, L. Bin, L. Jiajun, Y. Aiming, M.H.S.S. Ramakrishna, G. Matthew, R.C.N. Rao, P. Dravid, Vinayak, Adv. Mater. 24 (2012) 3549.
[14] B. Mukherjee, Y. Cai, H.R. Tan, Y.P. Feng, E.S. Tok, C.H. Sow, A.C.S. Appl, Mater. Interfaces 5 (2013) 9594.
[15] D. Wei, L. Yao, S. Yang, J. Hu, M. Cao, C. Hu, Inorg. Chem. Front. 2 (2015) 657.
[16] J. Lauth, F.E.S. Gorris, M. Samadi Khoshkhoo, T. Chassé, W. Friedrich, V. Lebedeva, A. Meyer, C. Klinke, A. Kornowski, M. Scheele, H. Weller, Chem. Mater. 28 (2016) 1728.
[17] D.A. Bandurin, A.V. Tyurnina, G.L. Yu, A. Mishchenko, V. Zólyomi, S.V. Morozov, R.K. Kumar, R.V. Gorbachev, Z.R. Kudrynskyi, S. Pezzini, Z.D. Kovalyuk, U. Zeitler, K.S. Novoselov, A. Patanè, L. Eaves, I.V. Grigorieva, V.I. Fal'ko, A.K. Geim, Y. Cao, Nat. Nanotechnol. 12 (2017) 223.
[18] Y. Cai, G. Zhang, Y.-W. Zhang, J. Phys. Chem. C 121 (2017) 10182.
[19] S.J. Magorrian, V. Zólyomi, V.I. Fal'ko, Phys. Rev. B 94 (2016) 245431.
[20] J.F. Sánchez-Royo, G. Mun¯oz-Matutano, M. Brotons-Gisbert, J.P. Martínez-Pastor, A. Segura, A. Cantarero, R. Mata, J. Canet-Ferrer, G. Tobias, E. Canadell, J. Marqués-Hueso, B.D. Gerardot, Nano Res. 7 (2014) 1556.
[21] Y. Sun, S. Luo, X.-G. Zhao, K. Biswas, S.-L. Li, L. Zhang, Nanoscale 10 (2018) 7991.
[22] G.W. Mudd, S.A. Svatek, T. Ren, A. Patane, O. Makarovsky, L. Eaves, P.H. Beton, Z.D. Kovalyuk, G.V. Lashkarev, Z.R. Kudrynskyi, A.I. Dmitriev, Adv. Mater. 25 (2013) 5714.
[23] S. Demirci, N. Avazli, E. Durgun, S. Cahangirov, Phys. Rev. B 95 (2017) 115409.
[24] T. Hu, J. Zhou, J. Dong, Phys. Chem. Chem. Phys. 19 (2017) 21722.
[25] T. Hu, J. Dong, Phys. Rev. B 92 (2015) 064114.
[26] Y. Zhang, B. Shang, L. Li, J. Lei, RSC Adv. 7 (2017) 30327.
[27] X.-P. Wang, X.-B. Li, N.-K. Chen, J.-H. Zhao, Q.-D. Chen, H.-B. Sun, Phys. Chem. Chem. Phys. 20 (2018) 6945.
[28] X. Li, C. Xia, J. Du, W. Xiong, J. Mater. Sci. 53 (2018) 3500.
[29] J.E. Padilha, R.H. Miwa, A.J.R. da Silva, A. Fazzio, Phys. Rev. B 95 (2017) 195143.
[30] Z. Chen, J. Biscaras, A. Shukla, Nanoscale 7 (2015) 5981.
[31] F. Yan, L. Zhao, A. Patan, P. Hu, X. Wei, W. Luo, D. Zhang, Q. Lv, Q. Feng, C. Shen, K. Chang, L. Eaves, K. Wang, Nanotechnology 28 (2017) 27LT01.
[32] K.D. Pham, N.N. Hieu, V.V. Ilyasov, H.V. Phuc, B.D. Hoi, E. Feddi, N.V. Thuan, C.V. Nguyen, Superlattices Microstruct. 122 (2018) 570.
[33] C.-X. Xia, J. Du, X.-W. Huang, W.-B. Xiao, W.-Q. Xiong, T.-X. Wang, Z.-M. Wei, Y. Jia, J.-J. Shi, J.-B. Li, Phys. Rev. B 97 (2018) 115416.
[34] P. Giannozzi, S. Baroni, N. Bonini, M. Calandra, R. Car, C. Cavazzoni, D. Ceresoli, G.L. Chiarotti, M. Cococcioni, I. Dabo, A.D. Corso, S. de Gironcoli, S. Fabris, G. Fratesi, R. Gebauer, U. Gerstmann, C. Gougoussis, A. Kokalj, M. Lazzeri, L. Martin-Samos, N. Marzari, F. Mauri, R. Mazzarello, S. Paolini, A. Pasquarello, L. Paulatto, C. Sbraccia, S. Scandolo, G. Sclauzero, A.P. Seitsonen, A. Smogunov, P. Umari, R.M. Wentzcovitch, J. Phys.: Condens. Matter 21 (2009) 395502.
[35] P.E. Blöchl, Phys. Rev. B 50 (1994) 17953.
[36] G. Kresse, D. Joubert, Phys. Rev. B 59 (1999) 1758.
[37] J.P. Perdew, K. Burke, M. Ernzerhof, Phys. Rev. Lett. 77 (1996) 3865.
[38] J.P. Perdew, K. Burke, M. Ernzerhof, Phys. Rev. Lett. 78 (1997) 1396.
[39] S. Grimme, J. Computat. Chem. 27 (2006) 1787.
[40] H. Jin, J. Li, Y. Dai, Y. Wei, Phys. Chem. Chem. Phys. 19 (2017) 4855.